

## Impact of the planetary boundary layer processes on the turbulent length scales and heat fluxes at surface

F. Lohou<sup>\*(1)</sup>, Said F.<sup>(1)</sup>, Lothon M.<sup>(1)</sup>, Durand P.<sup>(1)</sup>, Serca D.<sup>(1)</sup>, Ramier D.<sup>(2)</sup>, Cappelaere B.<sup>(2)</sup> and Boulain N.<sup>(2)</sup>

(1) Université de Toulouse, Laboratoire d'Aérodynamique - CNRS UMR 5560, Toulouse, France

(2) UMR HydroSciences, IRD, Montpellier, France

### 1. INTRODUCTION

The heat fluxes over continental surface quantify the heat exchanges between the surface and the air above. They depend on surface conditions but also on Atmospheric Boundary Layer (ABL) processes which modify the thermodynamical characteristics of the air. Among these ABL processes, entrainment of dry and warm air from the free troposphere into the ABL has a major importance. It leads to a warming and drying of the ABL air column which can modify the heat fluxes at the surface but also imposes its own scales to the scalar distribution. Whereas turbulent convection is characterized by very small spatial and temporal scales, the entrainment scales are larger and close to those of coherent thermal upward currents at the top of the ABL or of ABL clouds spatial distribution.

Using these scale differences between entrainment and turbulent convection, we try to determine which one of those processes drive the surface fluxes and scalar distribution near the surface. The spectral characteristics (integral length scale) and turbulent third-order moment (skewness) of wind velocity, temperature and water vapor mixing ratio measured by ground-based stations are analyzed in order to investigate the respective role of entrainment and turbulent convection near the surface.

This study leans on the AMMA experiment (African Monsoon Multidisciplinary Analyses, (Redelsperger et al., 2006). The West African Monsoon (WAM) is governed by the migration of the Inter Tropical Front (ITF) which is the interface between the moist southwesterly monsoon flow and the overlying dry Saharian Air Layer (SAL): it moves northward before the monsoon onset, and retreats southward at the end of the wet season (Sultan et al., 2007) . The experimental implementation at the surface in three meso-sites approximately along the 2°E latitudinal transect provides high rate thermodynamical and dynamical measurements during an entire annual cycle. The link between surface and the vertical structure of the low troposphere is made through UHF wind profiler and aircraft vertical exploration.

First, the seasonal meteorological context at two different latitudes near the surface is presented showing the impact of the ITF migration on the seasons shifting and duration at each site. After a careful check of our estimates, the seasonal variability of the integral scales of scalars and second order moment is linked to the ABL characteristics and reveals which processes prevail at the surface. Then an analysis of case studies at rain event and diurnal cycle time scales confirms the link between integral scales, skewness, heat fluxes and the sources of heat and humidity.

### 2. DATA SET AND METEOROLOGICAL CONTEXT

For this study, the high rate measurements of the three wind components ( $U, V, W$ ), temperature ( $t$ ) and water vapour mixing ratio  $r_v$ , made by two ground-stations are used. The first surface station was implemented by Laboratoire d'Aérodynamique in the Donga meso-site in North Benin, near the Nangatchori village (1°44.46 E, 9°38.84N). It lies within a Southern Sudanian vegetation-type zone characterized by woodland savannah. The second station is implemented by IRD (Institut de Recherche pour le Développement) further north in the semi-arid Niamey meso-site of Wankama, in a fallow field (2.4°E, 13.4°N) (Ramier et al., 2008). These ground-based stations belong to two of the three meso-sites along a latitudinal transect. A sonic anemometer and a Licor hygrometer were used on both stations and eddy-covariance method has been applied to process turbulent moments on 30 minutes samples over a seasonal cycle (September 2005 to September 2006).

At Benin meso-site, a 5-beam 915 MHz wind profiler from CNRM (Centre National de Recherche Météorologique) provided the vertical profiles of wind and reflectivity up to 5 km agl, with a 5 minutes and 150 m temporal and vertical resolutions. The back scattered power is proportional to the structure coefficient of the air refractive index  $C_n^2$  which increases in regions of large variability in temperature and humidity. The maximum of  $C_n^2$  over height gives an estimate of the height of the ABL top inversion. Surface stations and Wind profiler mea-

---

<sup>\*</sup>corresponding author address: Fabienne Lohou, Centre de Recherches Atmosphériques, 8 route de Lannemezan, 65300 Campistrous, France; email: lohfo@aero.obs-mip.fr

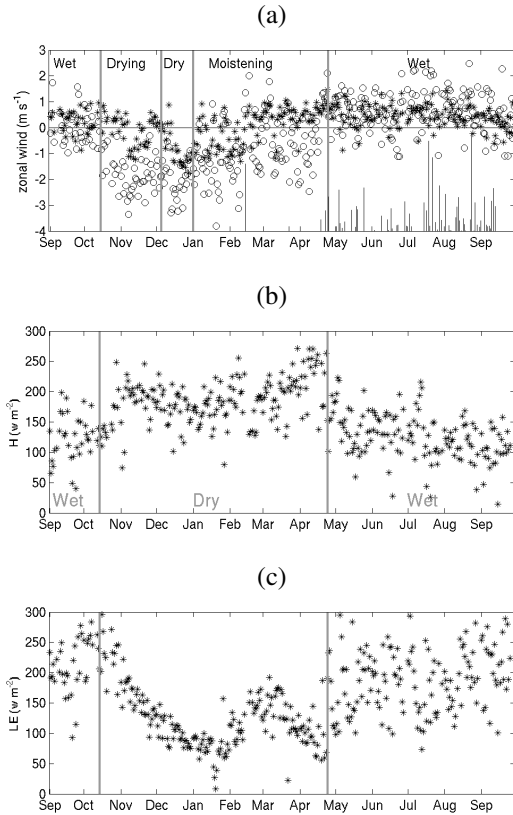


Figure 1: Seasonal view of (a) (\*) nighttime (0000-0600 UTC) and (o) daytime (1100-1700 UTC) zonal wind, (b) daytime H and (c) LE over the Benin meso-site of Nangatchori. Rain events are indicated by bars in panel (a).

Measurements were performed in the 2005-2007 Enhanced Observation Period.

During three Special Observation Periods (SOPs), from early June to mid August, the French ATR aircraft flew in Niamey area, providing fast measurements of wind, temperature and humidity. Each flight was composed of soundings and several 60 to 80 km stacked legs flown within and above the ABL.

The studied period, from September 2005 to September 2006, is presented in Fig. 1 and 2 with the nighttime (0000-0600 UTC) and daytime (1100-1700 UTC) zonal wind, the rain events and the daytime sensible (H) and latent (LE) heat fluxes in Nangatchori and Wankama respectively. The changes in the sign of the zonal wind mark the different periods established and discussed by Lothon et al. (2008b). The positive values correspond to the cold and moist monsoon flow whereas negative values indicate the warm and dry Harmattan flow. The annual cycle can be divided in four periods (Dry, Moistening, Wet and Drying) for both sites but with time shifts from one site to the other due to the ITD moving northward or

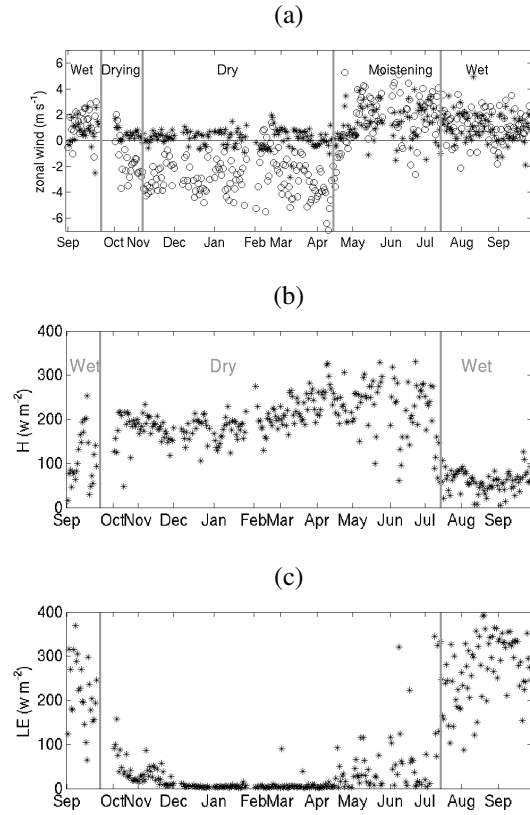


Figure 2: Same as Fig. 1 over the Niger meso-site of Wankama (After Ramier et al., 2008).

southward. The wet season in Nangatchori starts at the end of April with a well settled monsoon flow all day and first rain events. Further north, at Wankama, the monsoon onset determines the wet season start, around the 10<sup>th</sup> of July in 2006. The increase of the convection has about a 10-day delay in 2006 with respect to mean (Janicot and Sultan, 2007). The succession of those very different flows, with distinct rain amount, also result in an annual cycle of the heat fluxes. The annual variation at the Niger site is much sharper than at the Benin site where the vegetation activity along the whole year results in a slow decrease of LE after the wet season.

### 3. ESTIMATING INTEGRAL SCALES

The relative roles of the mixed-layer processes and the surface processes are analyzed through the integral scale of scalar and second-order moments. The integral scale can be interpreted as the size of the largest eddies of the inertial subrange. It is defined by the distance at which the signal is no longer correlated with itself and can be written as the integration of the autocorrelation func-

tion  $R_X(r)$  of the variable X:

$$l_X = \int_0^{\infty} R_X(r) dr. \quad (1)$$

$l_X$  is often estimated over a restricted integration from 0 to the first zero of  $R_X(r)$  (Lenschow and Stankov, 1986). Kaimal and Finnigan (1994) showed that this scale is related to the limit of the spectra at when the frequency  $f$  tends toward zero:

$$S_X(0) = \frac{4\overline{X^2}l_X}{U}. \quad (2)$$

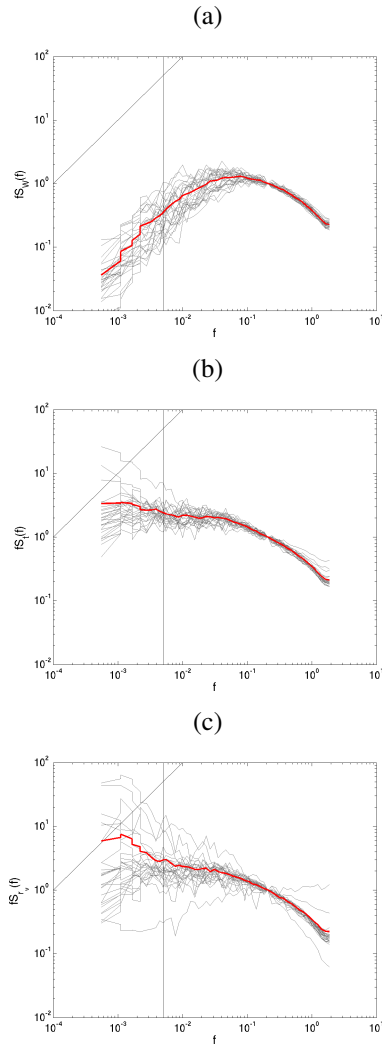


Figure 3: Daily normalized energy spectra (in gray) of (a)  $W$ , (b)  $t$  and (c)  $r_v$  for July 2006. The red line stands for the monthly averaged energy spectra.

So it is of primary importance, when estimating an integral scale, to be cautious about the existence of this limit and to check the shape of the spectra at low frequency.

Here we consider our measurements in the mixed layer and those made at the ground differently as regard this caution.

Few studies have dealt with the spectral shape in the convective boundary layer. Kaimal and Finnigan (1994) present a schematic representation of the evolution of spectra of velocity and temperature with height in the convective boundary layer. The spectra of wind converge at low frequencies, so that the integral scale can be defined. On the opposite, the spectra of temperature have a negative slope at low frequencies, making impossible the integral scale estimation. Using various lengths of aircraft times series, Durand et al. (2000) found increasing length scales from 40 m to more than 1000 m with increasing sample length from 11 km to 180 km for all scalars and second-order moments length scales for which  $W$  is not involved. Based on those results, and when using the aircraft measurements within the mixed layer, only  $l_W$  or  $l_{WX}$  are considered here.

For the surface measurements in Nangatchori, the spectral shape at low frequencies have been systematically verified. Figure 3 shows an exemple of the diurnal (1100-1700 UTC) average spectra  $fS(f)$  for  $W$ ,  $t$  and  $r_v$  in July 2006. These spectra are normalized by the  $fS_X(f)$  value at  $2 \cdot 10^{-2}$  Hz. Whereas  $W$  spectra nicely drop with a 1:1 slope towards low frequencies, the scalar spectra slope tend to highly varying values, not close to 1, at low frequencies. Therefore, the slope of  $fS_W(f)$ ,  $fS_{r_v}(f)$  and  $fS_t(f)$  over one decade (from  $5 \cdot 10^{-4}$  to  $5 \cdot 10^{-3}$  Hz) has been calculated for each 30-minutes sample and will be used as a convergence criterion.

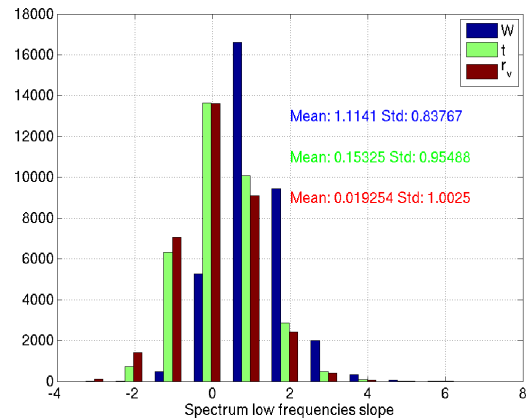


Figure 4: Distribution of the  $fS_W(f)$ ,  $fS_{r_v}(f)$  and  $fS_t(f)$  slopes at low frequencies for one year (Sept 05-Sept 06).

The annual distribution of the slopes at low frequencies obtained are displayed in Fig. 4. As expected,  $fS_W(f)$  has a slope of 1 in average, with a standard deviation

of 0.84. The mean values of only 0.15 and 0.02 for the slopes of respectively  $fS_t(f)$  and  $fS_{r_v}(f)$  confirm the need to check the spectra before estimating the integral scales. Based on the standard deviation of  $fS_w(f)$  slopes, we rejected  $fS_t(f)$  and  $fS_{r_v}(f)$  for which the slope is  $< 0.2$  or  $> 1.8$ . This was possible only at the Benin site, because the spectra for the Niger site were not available after the integral scale calculation. This point will be further discussed later.

#### 4. SEASONAL OVERVIEW OF THE INTEGRAL SCALE

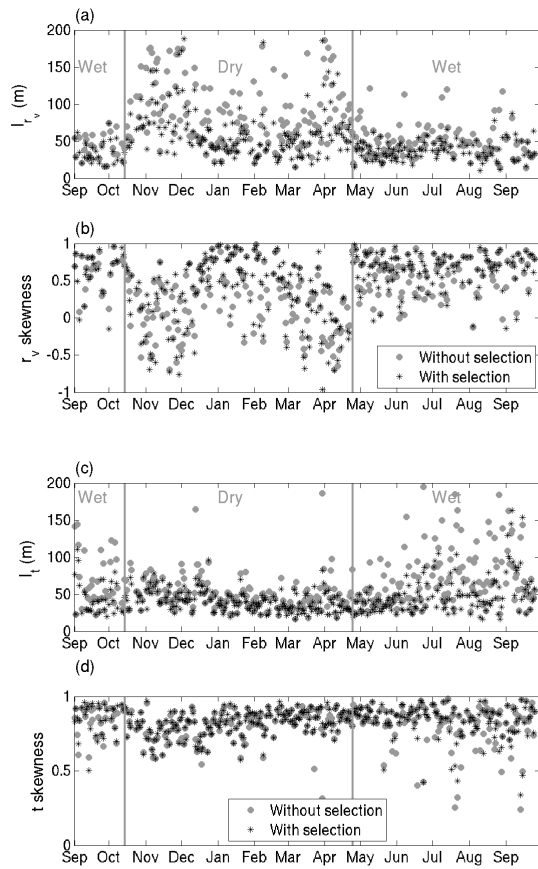


Figure 5: Time series of (a and b)  $r_v$  and (c and d)  $t$  integral scale and skewness over Nangatchori site from Sept. 2005 to Sept. 2006, (dark \*) with and (gray o) without spectra selection.

The temporal evolution of the diurnal average of integral scale and skewness of  $r_v$  and  $t$  for the whole annual cycle are presented in Fig. 5 with and without spectra selection for the Nangatchori site.  $l_{r_v}$  has a clear seasonal evolution with values smaller than 50 m during the

wet season, associated with positive skewness. Outside this period,  $l_{r_v}$  is more scattered and can reach 200 m in November and April. The associated skewness is close to zero and can be negative. Even if the seasonal signature on  $l_t$  appears less clearly, larger values are observed during the wet season. As expected, from thermal activity,  $t$  skewness near surface remains constant around 0.8. Note that the spectra selection made previously results in lower diurnal values of integral scale but does not change the seasonal variations. This allows us to present the same variables estimated over the Niger site but without spectra selection. As observed over the southern Benin site, large values of  $l_{r_v}$  associated with negative skewness occur during the dry season whereas low values of  $l_{r_v}$  with a positive skewness are observed during the wet season.

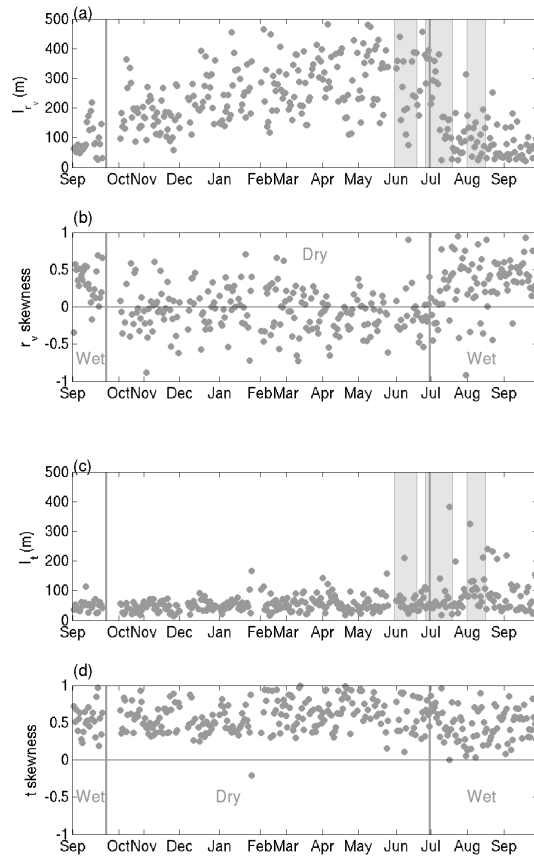


Figure 6: Time series of (a and b)  $r_v$  and (c and d)  $t$  integral scale and skewness over Niamey site from Sept. 05 to Sept. 06, without spectra selection. Gray zones indicate the SOPs time during which the French ATR aircraft flew over Niamey area.

These variations in spectral and turbulent characteristics of  $r_v$  and  $t$  along the year may indicate a temporal

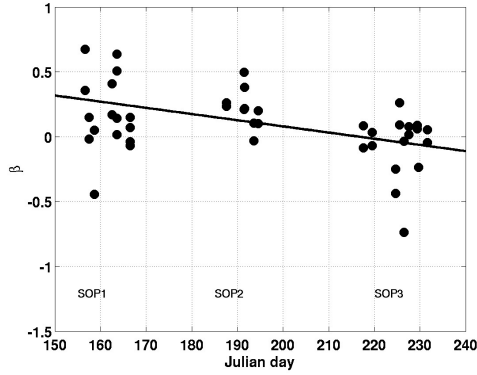


Figure 7: Ratio  $\beta$  of entrainment buoyancy flux to surface flux observed during the three probing periods of the ATR aircraft.

evolution of the ABL processes which impact on the surface. Dry and wet seasons present of course an opposite location of heat and humidity sources. During the wet season, the surface humidity source prevails and the turbulent convection of humid air leads to short  $l_{r_v}$  and positive skewness. On the contrary, outside this wet season, when convection of humid air from the surface decreases, the humidity repartition in the ABL down to the surface is governed by other processus like entrainment at the top of the boundary layer. This hypothesis is in agreement with larger  $l_{r_v}$  and negative skewness of  $r_v$  at that time.

Aircraft flights performed in the dry to wet transition period over Niamey area allow us to link our observations at surface at the Niger site with the processes occurring in the entire ABL, especially entrainment at the top. Estimates of the entrainment at the ABL top made with airborne measurements during AMMA experiment are shown in a companion paper by (Lothon et al., 2008a). Figure 7 gives the temporal evolution of the ratio  $\beta$  of entrainment buoyancy flux to surface buoyancy flux.

$$\beta = -\frac{\overline{W'\theta'_{vZI}}}{\overline{W'\theta'_{v0}}} \quad (3)$$

$\beta$  decreases with the ITD moving northward which is accompanied by a decreasing of the ABL height. The three periods of ATR flights considered in Fig. 7 are indicated in Fig. 6 (a and c) with gray areas, in order to highlight the impact of entrainment on the scalars at surface. We find that larger  $\beta$  are associated with larger  $l_{r_v}$  when the moist convection is reduced. During the wet season,  $\beta$  and  $l_{r_v}$  decrease. This is confirmed by the vertical profiles of  $l_{W_{r_v}}$ ,  $l_{W_t}$ ,  $S_{r_v}$  and  $S_t$  (Fig. 8) based on the aircraft measurements.  $l_{W_{r_v}}$  and  $l_{W_t}$  decrease within the whole ABL depth from early in the season to later, with decreasing  $\beta$ . However, we do not observe this at the surface (not shown here). These two second-order moment integral scale are imposed by the scales of  $W$ , which are always

small near the surface. The integral scale  $l_X$  of the scalar  $X$  depends on the scalar source location, and impacts on the strength of the surface scalar flux  $\overline{W'X'}$ . On the contrary,  $l_X$ , which is significantly larger than  $l_W$ , does not influence  $l_{WX}$  at the surface.

## 5. RESPECTIVE ROLE OF ABL PROCESSES AT RAIN EVENT AND DIURNAL TIME SCALES

The impact of the entrainment at the ABL top on scalar scale shown previously is now investigated at a rain event and diurnal time scales.

### 5.1 RAIN EVENT TIME SCALE

Figure 9 shows the evolution of the 1100-1700 UTC averaged evaporative fraction and  $l_{r_v}$  for a 13-day period in April. The evaporative fraction, after both of the 18<sup>th</sup> and 24<sup>th</sup> April rain events, decreases during several days. In the same time,  $l_{r_v}$  has an opposite behavior with small values right after the rain and increasing values as the soil dries up and the entrainment prevails.

Six rain events, occurring before monsoon onset in Nangatchori, are gathered in Fig. 10. This figure displays the evaporative fraction and  $l_{r_v}$  as a function of the number of days after rain. Values at day zero indicate the initial conditions measured before the rain whereas values at day 1 are acquired after the rain. The anti-correlation between  $l_{r_v}$  and evaporative fraction is confirmed, indicating that as soon as the surface humidity source decreases and is not sufficiently strong to drive  $r_v$  distribution near the surface, the entrainment imposes its own scale to the  $r_v$  distribution in the whole ABL depth down to the surface.

### 5.2 DIURNAL TIME SCALE

We are now looking at the impact of entrainment on the scalar scales and fluxes at the diurnal time scale.

The time-height section of the wind on the 20<sup>th</sup> of April shows a 1 km deep monsoon flow well settled all along the day, capped by the easterly wind of the SAL (Fig. 11 (a)). The ABL depth slightly increases, from 500 m to 1000 m, until 1300 UTC within the monsoon flow. Once the ABL height reaches the sheared layer between cold and moist monsoon and warm and dry easterlies above, it grows rapidly up to 2.5 km within two hours and half. The rain event of 18 April delayed the ABL growth and resulted in small Bowen ratio, though still larger than 1 until 1300 UTC (Fig. 11 (b)). When the ABL top reaches the sheared layer, it favours entrainment and intensifies the drying and warming of the ABL. The Bowen ratio decrease down to 1 for the rest of the day.

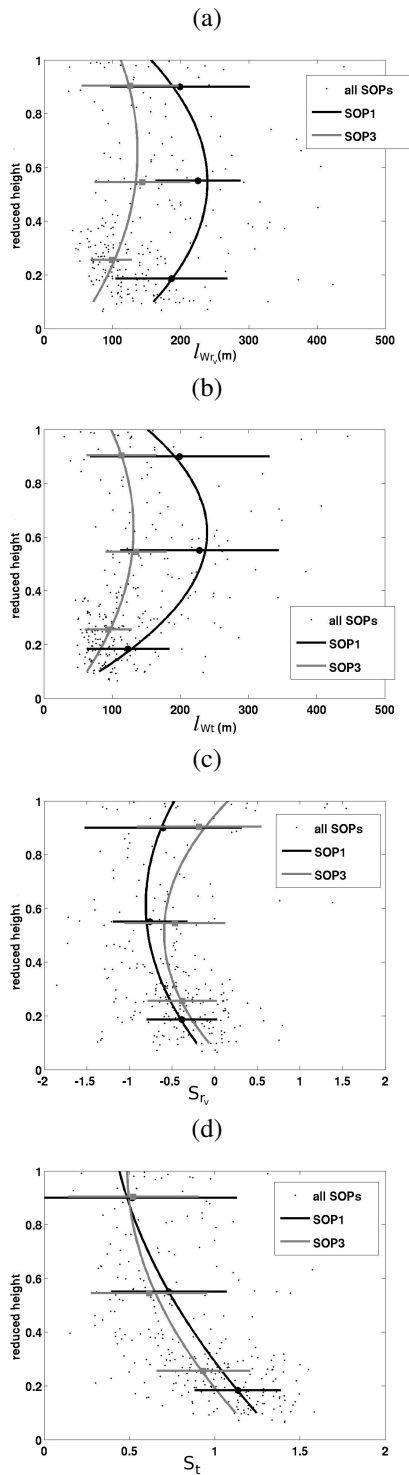


Figure 8: Vertical profiles of integral scales of second order moments (a)  $\overline{Wr}_v$ , (b)  $\overline{Wt}$  and skewness of (c)  $r_v$  and (d)  $t$  observed with aircraft. Second-order polynomial regressions are plotted for the first and third SOPs.

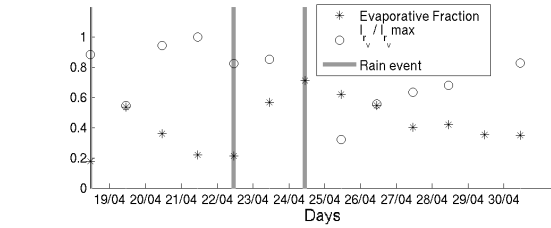


Figure 9: Temporal evolution of the 1100-1700 UTC averaged evaporative fraction and  $l_{r_v}$  for a 13-day period in April. Rain events are indicated by the vertical gray lines.

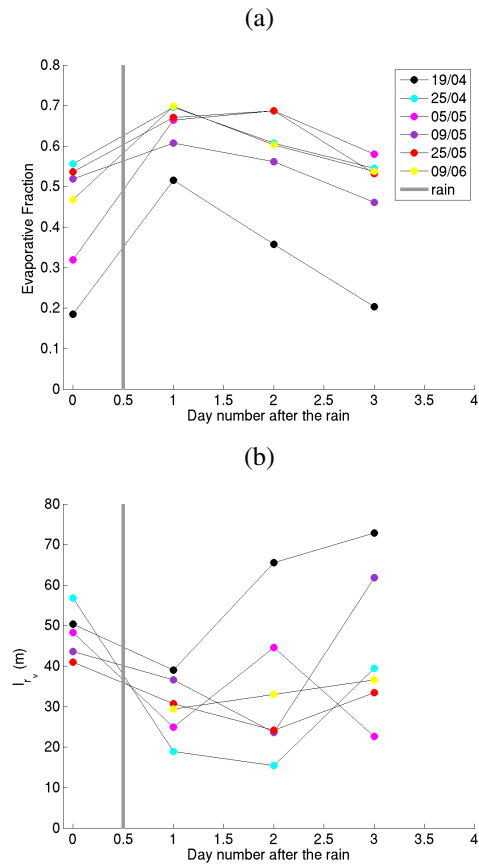


Figure 10: Temporal evolution of the evaporative fraction (a) and  $l_{r_v}$  (b) for several rain events in Nangatchori versus the day's number after the rain. Initial surface conditions are plotted at day zero and conditions just after the rain are plotted at day 1. The rain event occurred in between day zero and 1.

The impact of the ABL vertical development on the surface is also clearly seen on the integral scales and skewness of  $r_v$  and  $t$  (fig. 11 (c) and (d)) measured at the ground. The small values of  $l_{r_v}$  and  $l_t$  until 1300 UTC expressed the surface turbulent convection. In fact as long as the ABL develops within the monsoon flow, the sources of heat and humidity are mainly at the surface. At 1300 UTC, the ABL reaches the sheared layer, increasing the role of the sources of heat and dry air at the top. This entrainment of warm and dry air within the boundary layer reaches the surface and imposes its own scale on  $r_v$  and  $t$ , so that larger integral scales, negative skewness of  $r_v$  and lower bowen ratio are observed.

## 6. CONCLUSION

In the West African Monsoon context, the succession of dry and wet seasons leads to contrasting surface conditions at the lower limit of the atmospheric boundary layer. Moreover, entrainment processes at the upper limit can occur in a very sheared layer between cold moist monsoon and warm dry Harmattan flows. Therefore sources of heat and humidity can be both at surface or ABL top.

The impact of turbulent convection and entrainment on the surface heat fluxes and distribution of humidity and temperature near the surface has been studied through the integral scales and skewness estimated from high rate measurements at surface. When the surface source prevails, small integral scales associated with positive skewness can be observed. On the opposite, when the top ABL source prevails, entrainment imposes its own larger scale and leads to important integral scales with negative skewness for humidity. This can be observed on seasonal cycle but also between rain events before the monsoon onset when they are sufficiently sparse to allow the drying at surface. The reversal of the sources can also occur at the diurnal time scale. Turbulent convection imposes its scale while the boundary layer develops within the monsoon flow. As soon as it reaches the sheared layer, the entrainment modifies the Bowen ratio and the scalar distribution near the surface.

### Acknowledgements

Based on a French initiative, AMMA was built by an international scientific group and is currently funded by a large number of agencies, especially from France, UK, US and Africa. It has been the beneficiary of a major financial contribution from the European Community's Sixth Frame-Newsletter AMMA-France 06/12/2006 work Research Programme.

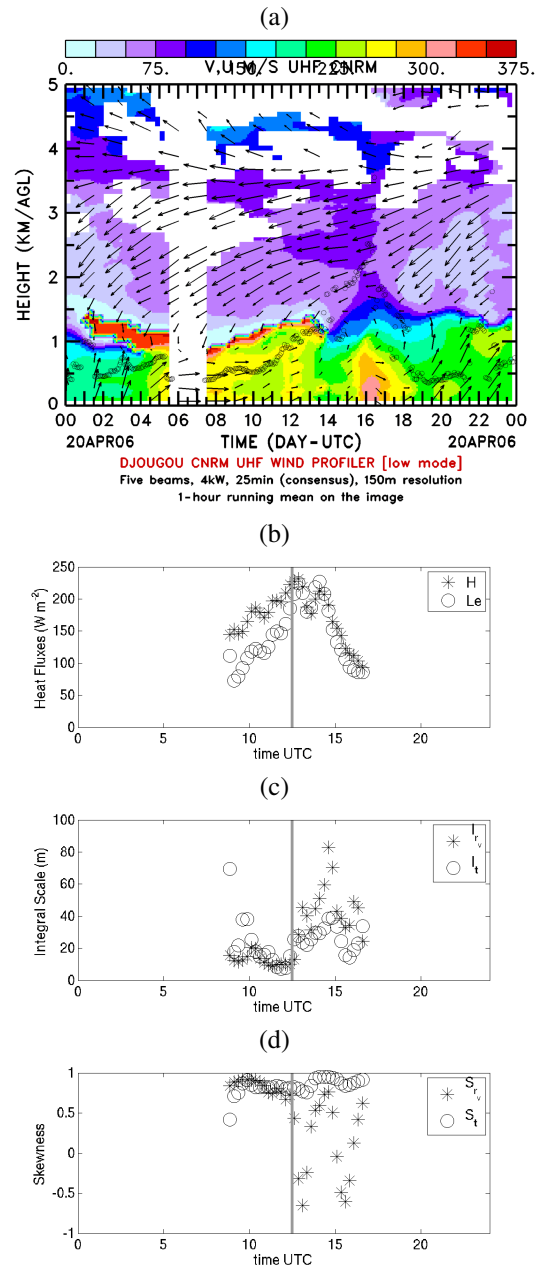


Figure 11: Time height section of wind with ABL depth (dots) measured by UHF wind profiler in Nangatchori on 20<sup>th</sup> of April 2006 (a). Diurnal evolution of heat fluxes H and LE (b), integral scales (c) and skewness (d) of  $r_v$  and  $t$  for the same day at the surface.

## REFERENCES

- Durand, P., F. Thoumieux, and D. Lambert, 2000: Turbulent length-scales in the marine atmospheric mixed layer, *Quart. J. Roy. Meteor. Soc.*, **126**, 1889–1912.
- Janicot, S. and B. Sultan, 2007: The large-scale context of the West African Monsoon in 2006, *Exchanges CLIVAR newsletter*, **12**, **2**, 11–17.
- Kaimal, J. C. and J. J. Finnigan, 1994: *Atmospheric Boundary Layer Flows*, Oxford University Press.
- Lenschow, D. H. and B. B. Stankov, 1986: Length scales in the convective boundary layer, *J. Atmos. Sci.*, **43**, 1198–1209.
- Lothon, M., G. Canut, F. SAID, F. Guichard, F. Couvreur, F. Lohou, and B. Campistron, 2008a: Processes involved in the planetary boundary layer in the frame of the west african monsoon, *18 Conference on Boundary Layer and Turbulence*.
- Lothon, M., F. Said, F. Lohou, and B. Campistron, 2008b: Diurnal cycle in the low troposphere of west africa and impact on the transport of water vapor, *MWR*, *in press*, **121**, 521-536.
- Ramier, D., N. Boulain, B. Cappelaere, F. Timouk, M. Rabanit, C. R. Lloyd, S. Boubkraoui, F. Métayer, L. Descroix, and V. Wawrzyniak, 2008: Towards an understanding of coupled physical and biological processes in the cultivated sahel- 1. energy and water, *submitted to J. Hydrol.*
- Redelsperger, J., C. Thorncroft, A. Diedhiou, T. Lebel, D. J. Parker, and J. Polcher, 2006: African Monsoon Multidisciplinary Analysis (AMMA): An international research project and field campaign, *Bull. Amer. Meteor. Soc.*, **87**, 1739–1746.
- Sultan, B., S. Janicot, and P. Drobinski, 2007: Characterization of the diurnal cycle of the West African Monsoon around the monsoon onset, *J. Climate*, **20**, 4014–4032.